

# SELF-AMORPHIZATION WITH CLUSTER IMPLANTATION

**K. Sekar, W. A. Krull, T. N. Horsky, and D. C. Jacobson**

*SemEquip, Inc., 34 Sullivan Road, N. Billerica, MA 01862 USA*

**K. Jones**

*Department of Materials Science and Engineering, University of Florida,  
Gainesville, FL, 32611*

**D. Henke**

*Qimonda Dresden GmbH & Co. OHG, P. O. Box 10 09 40,  
D-01079 Dresden, Germany*

A pre-amorphization implant (PAI) step is typically used to avoid crystal channeling and thus achieving shallower junctions. Octadecaborane ( $B_{18}H_{22}$ ), enables very low energy boron implant processes for the formation of very shallow p-type junctions and effectively amorphizes the silicon eliminating the need for a PAI. The goal of this work is to provide an analysis of the self-amorphization mechanism and to compare a variety of cluster ion species with regard to their self-amorphization. SIMS profiles as a function of implant dose are presented. These data provide strong evidence for the elimination of channeling as the implant progresses and the silicon becomes amorphous. Additional confirmation is provided by the use of a subsequent channeling-sensitive 200keV  $P^+$  implant to show the threshold of channeling avoidance. XTEM is also used to show the physical structure of the material as a function of implant dose and correlate with the channeling behavior.

## INTRODUCTION

The passage of an energetic ion through the Si lattice initiates a sequence of displacement events that leads to defect production. At sufficiently high doses, the crystalline silicon undergoes a crystalline-amorphous (*c-a*) transformation. In Si, amorphization occurs under ion irradiation when the free energy of the damaged crystalline phase is higher than that of the amorphous phase. Post-implant thermal processing is required to anneal out the damage and to electrically activate the introduced dopants. The formation of the amorphous phase also inhibits ion channeling and thus eliminates the channeling tail that one normally observes in a dopant profile. The process of amorphization depends on various factors like ion implant species [1], implant dose [2] and substrate temperature [3].

There are differences in the degree of damage created by lighter ions and heavier ions or heavy cluster ion species. The amorphous layer created by heavy ion damage can be regrown easily in silicon resulting in relatively efficient dopant activation. In the case of lighter ions it is difficult to produce an amorphous layer below a certain dose, and the defects formed in such cases are comparatively stable; hence the dopant activation is affected. For example, B implanted into pre-amorphized Si can achieve high activation levels during regrowth at low annealing temperatures [4]. The simultaneous observation of different characteristics during annealing for B in preamorphized Si and B in highly damaged crystalline Si can be clearly seen in the experiment of Jones *et al* [5].

Moreover, when the substrate is amorphous, low temperature anneals such as SPE provides a good opportunity to repair the damage and activate the dopants efficiently. Interstitials and vacancies recombine and the excess interstitials form clusters of {311} defects near 800°C. Below a certain damage threshold these {311} defects easily dissolve at a suitable anneal temperatures. Above a different damage threshold these defects can form dislocation loops that are difficult to remove. The use of ore-

amorphization implants (PAI) produces a high activation level with a low thermal budget, and therefore, with minimal diffusion. [6, 7]. It has been reported that during the regrowth of an amorphous layer, B atoms are incorporated into substitutional positions and thus become electrically active [8] at least for concentrations lower than  $10^{20}$  atoms/cm<sup>3</sup>. At the same time, the excess or deficiency of atoms existing in the amorphous layer that extends to the surface are swept towards the surface where they are annihilated. Only damage beyond the amorphous/crystalline interface remains after regrowth, which evolve into Si-interstitial clusters, {113} defects, and dislocation loops. Therefore, we can assume for simplicity that just after the regrowth, all B atoms within the amorphous region are in substitutional positions, and defects are removed from that region, while in the crystalline region B atoms interact with Si interstitials generated by the PAI.

Recently, the use of molecular or “cluster” implantation has enabled dopant-bearing molecules (such as B<sub>18</sub>H<sub>22</sub>) and carbon-bearing molecules (such as C<sub>16</sub>H<sub>10</sub>, C<sub>14</sub>H<sub>x</sub>) to increase throughput [9] and decrease implantation depth for certain USJ PMOS applications. It has been shown that a carbon cluster (C<sub>16</sub>H<sub>x</sub>) implant could be used to reduce boron diffusion. Combination of C<sub>16</sub>H<sub>x</sub>, B<sub>18</sub>H<sub>x</sub> and conventional spike annealing technologies are shown to produce ultra-shallow junctions appropriate for the 45nm SDE [10]. The important parameter that is crucial in obtaining the such shallow junction is the self-amorphizing nature of both C<sub>16</sub>H<sub>10</sub> and B<sub>18</sub>H<sub>22</sub> implants. Similar to a carbon cluster and a boron cluster combination implants, we believe that a carbon cluster with Arsenic tetramer (As<sub>4</sub>) and Phosphorous tetramer (P<sub>4</sub>) will produce similar effects on the diffusion of n-type dopants. Since boron and carbon cluster implantation are becoming mainstream manufacturing processes, it is therefore important to characterize the self-amorphization effects of B<sub>18</sub>H<sub>22</sub> and C<sub>16</sub>H<sub>10</sub> and look at the possibility to eliminate standard PAI implants to avoid channeling effect and EOR damage resulting in low damage high quality junctions [11].

The goal of this paper is to show the amorphizing properties of various cluster species and to evaluate the amorphous layer depth using XTEM measurements. We used a channeling sensitive implant (P<sup>+</sup>, 200keV, 1e14 atoms/cm<sup>2</sup>) to probe the degree of damage by B<sub>18</sub>H<sub>22</sub> implants (500eV and 5keV per boron atom) at various doses and correlate the results with XTEM measurements. This study will shed some light on the role played by amorphization in dopant activation for both USJ and stress engineering applications.

## EXPERIMENTAL

Wafers used in this study were 200mm, n-type, (100) silicon substrates. The wafers were implanted with various cluster species at different energies and doses using B<sub>18</sub>H<sub>x</sub><sup>+</sup>, C<sub>16</sub>H<sub>x</sub><sup>+</sup>, C<sub>7</sub>H<sub>x</sub><sup>+</sup> ions from a ClusterIon<sup>®</sup> source. TW measurements were performed on the as-implanted wafers before performing SIMS and XTEM measurements. The samples were imaged on a JEOL 2010 FEG TEM using on-axis multi beam imaging conditions.

## RESULTS AND ANALYSIS

### CLUSTERBORON

Fig. 1 (a), (b) and (c) shows XTEM images of B<sub>18</sub>H<sub>22</sub> 500eV per boron atom implant at doses 5e13, 1e14 and 1e15 atoms/cm<sup>2</sup> respectively. For 5e13 dose XTEM image (Fig 1(a)), there is no evidence for the presence of amorphous layer. For the 1e14 dose, one can see clearly amorphous pockets that are 3nm deep. At 1e15 dose there is a clear presence of an amorphous layer roughly about 6.2nm thick. This amorphous layer depth is roughly the sum ( $R_p + \Delta R_p$ ) of projected range ( $R_p$ ) and the straggle ( $\Delta R_p$ ) for boron at 500eV.

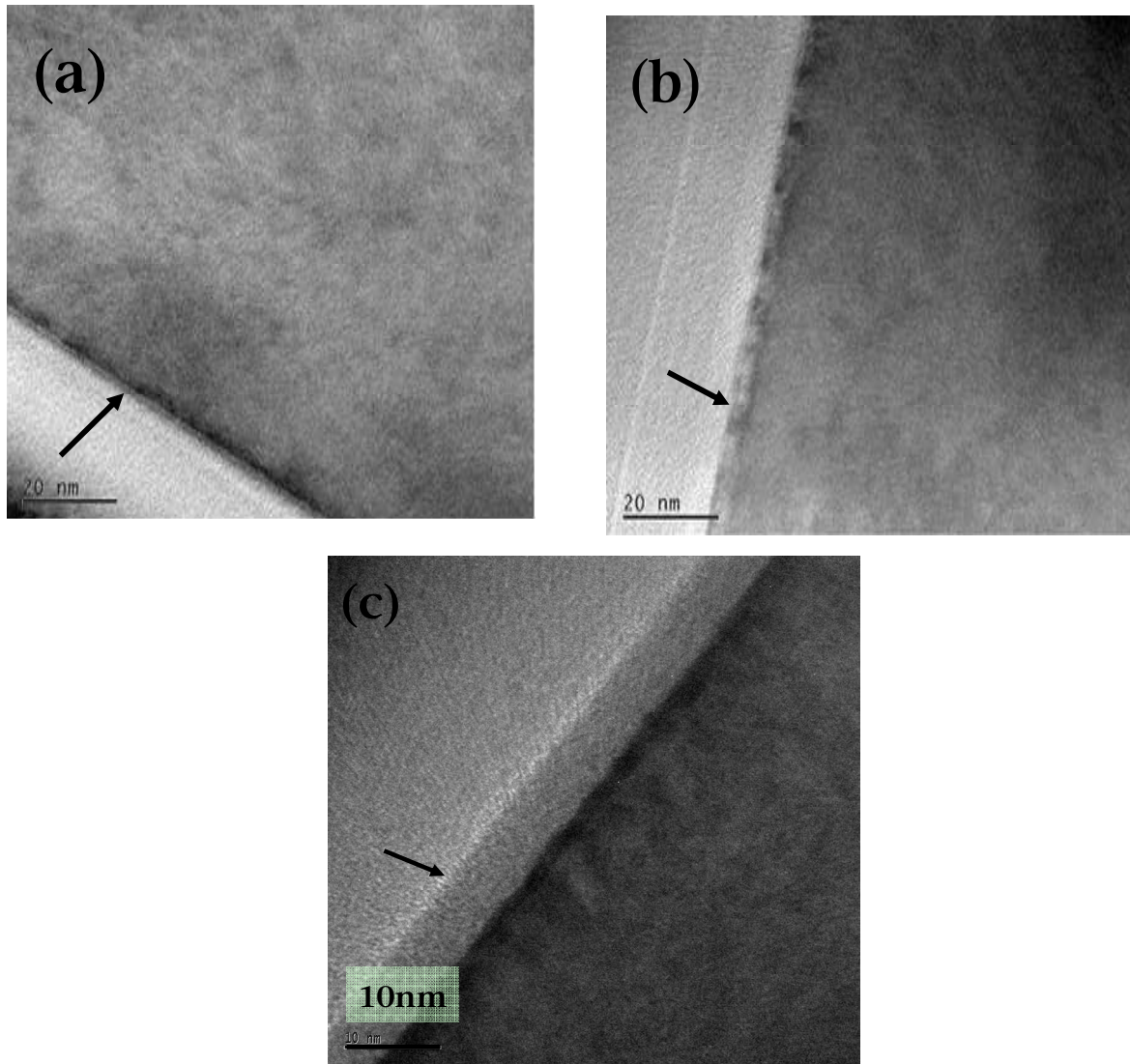


Fig. 1 shows a 500eV per boron atom implant at (a)  $5 \times 10^{13}$  atoms/cm<sup>2</sup> (no amorphous layer) (b)  $1 \times 10^{14}$  atoms/cm<sup>2</sup> (3nm deep amorphous pockets) (c)  $1 \times 10^{15}$  atoms/cm<sup>2</sup> (6.2nm thick amorphous layer). The arrow indicates the position of the surface.

To evaluate the threshold dose for amorphization,  $B_{18}H_{22}$  was implanted at 0.5keV and 5keV (per boron atom) at various doses from  $1 \times 10^{13}$  to  $1 \times 10^{15}$  atoms/cm<sup>2</sup>, and a channeling sensitive  $P^+$ , 200keV,  $1 \times 10^{14}$  implant was performed at 0° tilt and 0° twist on those wafers to determine the degree of damage created by the  $B_{18}H_{22}$  implants. It is expected that P will penetrate deeper in crystalline Si and shallower in amorphous Si. SIMS measurements were carried out to determine P profile and from the profile determined the critical dose for amorphization threshold. Figs. 2(a) and 2(b) shows the P SIMS profile on the samples implanted with 0.5keV and 5.0keV per boron atom  $B_{18}H_{22}$  at various doses. From Fig. 2(a) it is seen that the P profile is different for  $B_{18}H_{22}$  implant with  $1 \times 10^{13}$  and  $1 \times 10^{15}$  dose. The depth at P concentration of  $1 \times 10^{17}$  atoms/cm<sup>3</sup> for  $1 \times 10^{13}$  dose is around 0.9μm and for  $1 \times 10^{15}$  it is 0.7μm. The deeper profile for  $1 \times 10^{13}$  is likely due to the steering of P atoms in crystalline Si. Since such a low implant dose does not produce any appreciable damage, the P implant undergoes channeling and travels deeper into the crystal. At a  $1 \times 10^{15}$  dose it is shown that  $B_{18}H_{22}$  creates an amorphous layer depth of 6.2nm (Fig. 1(c)). The presence of an amorphous layer on the top of the crystalline Si dechannels the impinging P atoms

and thus steers them away from the channel. These steered away atoms undergo multiple random collisions with Si atoms and lose energy before coming to rest at a relatively shallower depth when compared to a case with a crystalline one. At a dose of  $5 \times 10^{13}$ , the depth of P profile at  $1 \times 10^{17}$  atoms/cm<sup>3</sup> is already close to  $0.8 \mu\text{m}$ . This is roughly half the decrease in depth when compared to a completely amorphous case. Even at a  $\text{B}_{18}\text{H}_{22}$  dose of  $5 \times 10^{13}$ , there is an appreciable degree of crystalline damage in Si. If one looks at the XTEM image at  $5 \times 10^{13}$  dose in Fig. 1(a), there is no clear evidence for the presence of any amorphous layer. At a dose of  $1 \times 10^{14}$  (Fig. 1(b)), XTEM shows a discontinuous 3nm deep layer of amorphous pockets. XTEM is not sensitive enough to pick up partially amorphized Si or deficiently recrystallized phase. Yoshimoto et al (12) have reported XTEM and Raman measurements on flash annealed boron samples where they claim that XTEM could not pick up deficiently recrystallized phase, whereas Raman measurements clearly showed deficiently recrystallized phase. These results indicate that to avoid channeling effect at this energy range, we do not need a higher dose of ClusterBoron than  $5 \times 10^{14}$  atoms/cm<sup>2</sup>.

Fig. 3 shows the boron differential profile for 0.5keV per boron atom  $\text{B}_{18}\text{H}_{22}$  implants. All the boron profiles were smoothed by doing a 5 point averaging and normalized with respect to  $1 \times 10^{13}$  profile. The differential SIMS profile was made by subtracting profiles. For example, the profile entitled “ $2 \times 10^{13} - 1 \times 10^{13}$ ” is obtained by subtracting the SIMS profile from a  $1 \times 10^{13}$  dose from the profile from a  $2 \times 10^{13}$  dose. Fig. 3 shows the incremental boron concentration for various doses. It is clear that we can observe the channeling tail up to  $5 \times 10^{13}$  dose. Beyond  $5 \times 10^{13}$  there is practically no difference in the boron profile below a concentration of  $1 \times 10^{17}$  atoms/cm<sup>3</sup>. This indicates that threshold dose for amorphization at 0.5keV  $\text{B}_{18}\text{H}_{22}$  implant is around  $5 \times 10^{13}$  atoms/cm<sup>2</sup>. Fig. 4 shows the P profile for the 5keV  $\text{B}_{18}\text{H}_{22}$  implant. While the threshold for amorphization is still around  $5 \times 10^{13}$  atoms/cm<sup>2</sup> it is not as clearly evident as in the case of 0.5keV per boron atom implants.

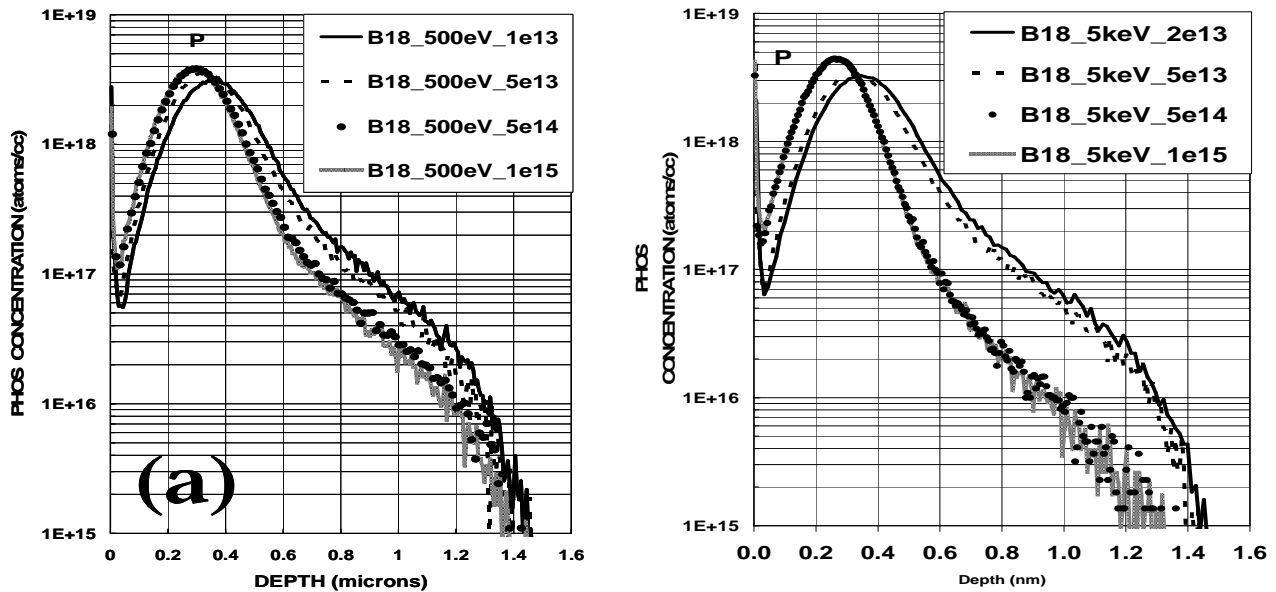


Fig. 2: SIMS profile for P+, 200keV,  $1 \times 10^{14}$  at  $0^\circ$  tilt and  $0^\circ$  twist.

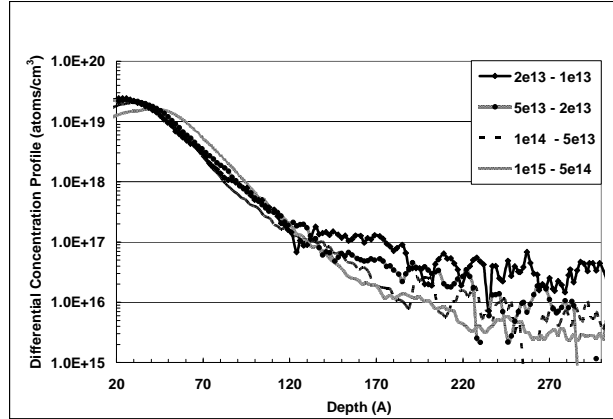


Fig. 3: Differential boron SIMS profile for  $B_{18}H_{22}$  at 0.5keV implanted at various doses.

### CLUSTERCARBON™

A new cluster species,  $C_{16}H_{10}$ , was previously discussed [10] for low energy carbon implant. By appropriate choice of hydrocarbon molecule, we have a molecule whose physical properties are very similar to  $B_{18}H_{22}$ . The  $C_{16}H_{10}$  chemical is also a solid at room temperature and vaporizes in the same temperature range as ClusterBoron. The soft ionization system developed for ClusterBoron also works very well for the  $C_{16}H_{10}$  vapor, which produces slightly higher electrical beam currents due to the narrower AMU spectrum of ClusterCarbon. In addition, the  $C_{16}H_x^+$  ion is in the same AMU range as ClusterBoron ( $\sim 200$ AMU) and so the remainder of the implant system works the same as with ClusterBoron. It is shown that ClusterCarbon inhibits boron diffusion during the anneal process, consistent with other developments using monomer carbon. Further, the combination of ClusterCarbon, ClusterBoron and conventional spike annealing technologies are shown to produce ultra-shallow junctions appropriate for the 45nm SDE. We have also another carbon cluster material ( $C_{14}H_x$ ) that can provide  $C_7H_y$  molecule. With a lower AMU the carbon equivalent energy can be pushed higher to enable deeper ClusterCarbon implants. Based on these results it becomes necessary to characterize the self-amorphizing properties of these ClusterCarbon species. Here we report XTEM results for the amorphous layer depth created by these species at few implant energies and doses.

It has been shown that 2 – 3 keV per carbon atom with a dose around  $1e15$  atoms/cm<sup>2</sup> is appropriate to use as a diffusion controlling implant with low energy (0.5keV) boron implants. So it is relevant to show the results of the amorphous layer depth created by carbon cluster species ( $C_{16}H_{10}$  and  $C_7H_x$ ) at those energies and dose. Fig 4(a) & 4(b) shows XTEM images of 3keV & 2keV per carbon atom  $C_{16}H_x$  implants at a dose of  $1e15$  atoms/cm<sup>2</sup>. The amorphous layer depths at 3keV & 2keV are around 14nm & 12nm respectively at a dose of  $1e15$  atoms/cm<sup>2</sup>. The amorphous layer depth created are well above the  $R_p$  of 0.5keV boron equivalent implant energies ( $R_p = 3.4$ nm,  $\Delta R_p = 2.9$ nm) and the whole boron profile is well within the amorphous layer created by the carbon cluster implants.

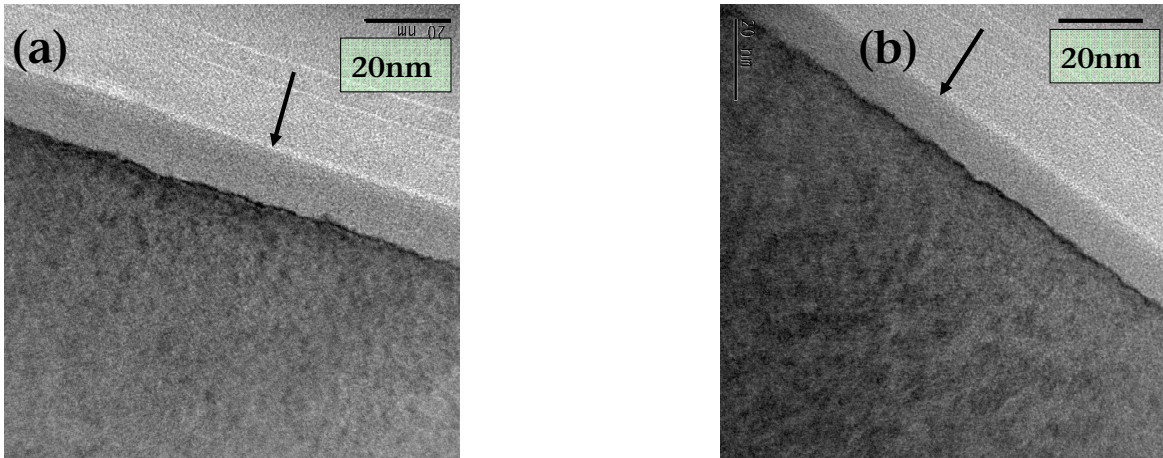


Fig. 4 shows XTEM images of  $C_{16}H_x$  implant at  $1e15$  atoms/cm<sup>2</sup> at (a) 3keV per carbon atom & (b) 2keV per carbon atom. The amorphous layer depth at 3 & 2keV are 14nm and 12nm, respectively. The arrow indicates the surface position.

Carbon cluster implant with  $C_7H_x$  species at 10keV per carbon atom showed no amorphous layer at  $3e14$  dose. Fig 5(a) shows XTEM image at  $3e14$  dose. Similar to  $B_{18}H_{22}$  implant where the channeling sensitive  $P^+$ , 200keV implant showed some degree of crystal damage even around  $5e13$  dose, we believe that for  $C_7H_x$  implant at  $3e14$  dose, there is some degree of crystal damage that is not detected by XTEM. At  $2e15$  dose Fig 5(b) we see a very clean amorphous layer (~26 nm). This amorphous layer depth is very crucial in activating the dopants i.e. placing the carbon atoms in substitutional site. Such activation is the key factor in producing stress in Si lattice.

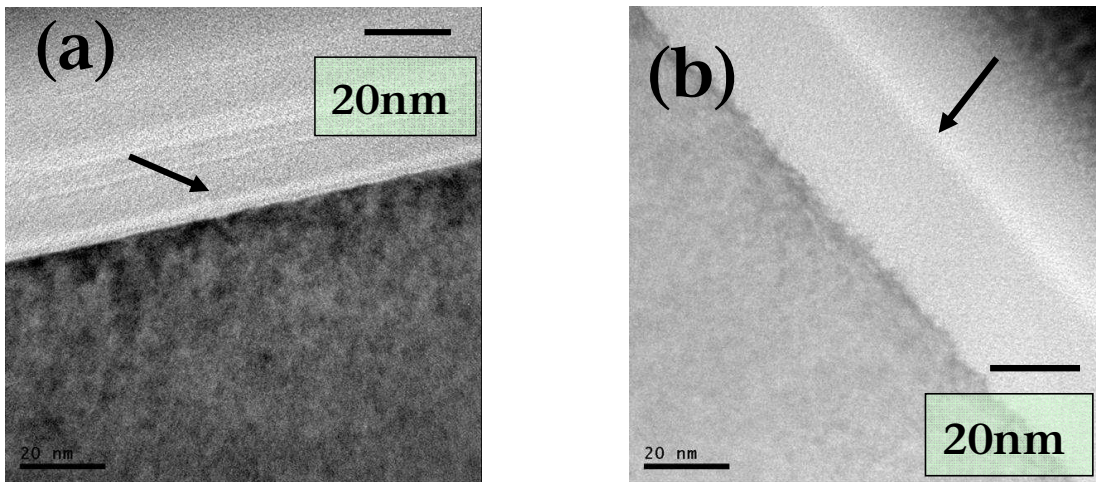


Fig. 5 shows XTEM images of  $C_7H_x$  implant at 10keV per carbon atom at (a)  $3e14$  atoms/cm<sup>2</sup> & (b)  $2e15$  atoms/cm<sup>2</sup>. The arrow indicates the surface position.

Fig 6 shows amorphous layer thickness at various doses for few energies of  $C_{16}H_x$  and  $C_7H_x$  species. Comparing the amorphous layer depth produced by  $C_{16}H_x$  and  $C_7H_x$  species at same equivalent carbon energies, it is clear that  $C_{16}H_x$  produces a larger amorphous depth when compared to  $C_7H_x$ . This difference is basically coming from the heavier mass of  $C_{16}H_x$ . Comparing  $C_7H_x$  at same dose but at different energies, we see a greater amorphous layer depth for higher energy. This follows from the deeper projected range and higher lateral straggle.

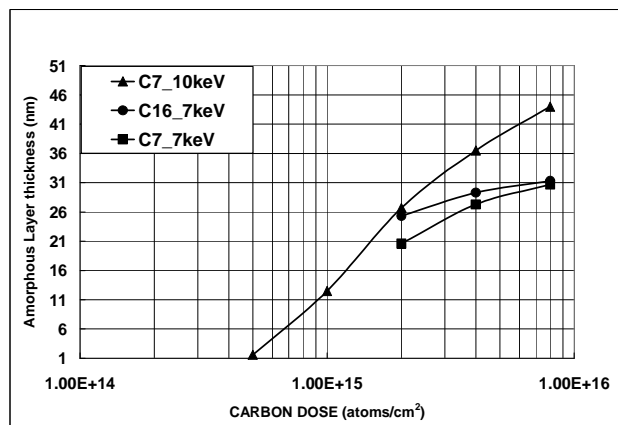


Fig. 6 shows amorphous layer depth vs carbon dose (from XTEM) for various energies and doses for  $C_7H_x$  and  $C_{16}H_x$ .

## CONCLUSIONS

$B_{18}H_x^+$ ,  $C_{16}H_x^+$  and  $C_7H_x^+$  ion cluster species show self-amorphizing properties that eliminate the need for a PAI implant. Using the channeling-sensitive 200keV  $P^+$  implant it is found that even at a boron dose of  $5e13$  atoms/cm<sup>2</sup>, there is sufficient crystal damage to reduce channeling effects. At a dose of  $5e14$  atoms/cm<sup>2</sup>, the degree of damage is enough to avoid channeling. The amorphous layer depth produced by  $C_{16}H_x$  is greater than the depth produced by  $C_7H_x$  species owing to the heavier mass for the former. The amorphous layer depth determined for various energies and doses for carbon cluster ions ( $C_{16}H_x^+$ ,  $C_7H_x^+$ ) will prove useful for applications that require amorphization and activation.

## ACKNOWLEDGMENTS

We would like to thank our GSD implant group Brian Haslam, Dennis Klesel and Jeff Buda for carrying out the implants.

## REFERENCES

- (1) T. Mootoka, O. W. Holland, Appl. Phys. Lett. **61**, 3005 (1992)
- (2) T. Mootoka, O. W. Holland, Appl. Phys. Lett. **58**, 2360 (1991)
- (3) T. Mootoka, F. Kobayashi, P. Fons, T. Tokuyama, T. Suzuki, N. Natsuaki, Jap. J. Appl. Phys. **30**, 3617 (1991)
- (4) E. Landi, A. Armigliato, S. Solmi, R. Köghler, and E. Wieser, Appl. Phys. A **A47**, 359 (1988).
- (5) K. S. Jones, R. G. Elliman, M. M. Petracic, and P. Kringhoj, Appl. Phys. Lett. **68**, 3111 (1996).
- (6) E. Landi, A. Armigliato, S. Solmi, R. Köghler, and E. Wieser, Appl. Phys. A **A47**, 359 (1988).
- (7) S. Solmi, E. Landi, and F. Baruffaldi, J. Appl. Phys. **68**, 3250 (1990).
- (8) O. W. Holland, J. Narayan, D. Fathy, and S. R. Wilson, J. Appl. Phys. **59**, 905 (1986)
- (9) D. R. Tieger, W. Divergilio, E. C. Eisner, M. Harris, T. J. Hsieh, J. Miranda, W. P. Reynolds, T. Horsky, Proc. 16<sup>th</sup> International Conference on Ion Implantation Technology, p206 (2006)
- (10) W. A. Krull, B. Haslam, T. Horsky, K. Venheyden, K. Funk, Proc. 16<sup>th</sup> International Conference on Ion Implantation Technology, p142 (2006)
- (11). J. Borland, M. Tanjo, N. Nagai, T. Aoyama and D. Jacobson, Semiconductor International, 52 (2005)
- (12) M. Yoshimoto et al, J. Electro. Chem. Soc, **153** G697 (2006)